# Technical insights into advanced numerical methods applied in 3D EM modelling

Paula Rulff, Laura Maria Buntin, Michael Weiss

Department of Earth Sciences
Uppsala University

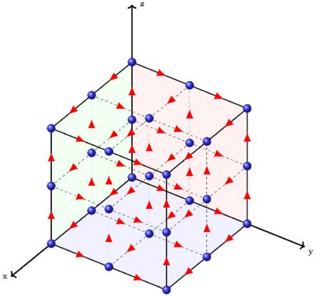


**EMinar**
1 March 2023

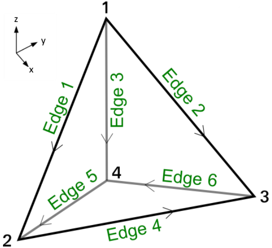

# MT & CSEM methods in frequency domain

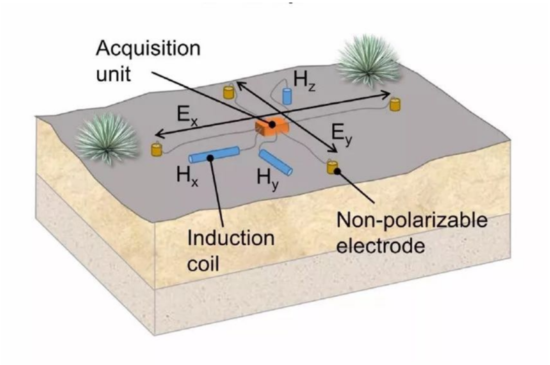


Receiver station setup (Bücker et al., 2017) for land-based MT and CSEM measurements.

**Magnetotellurics (MT) & Audiomagnetotellurics (AMT)**

Natural sources

f: $\approx 10^{-4} - 10^{4}$ Hz

Far-field assumption (plane waves)

Modelling: Source is impressed at domain boundaries or at anomalies

**Controlled-source electromagnetics (CSEM)**

Artificial sources

f: $\approx 10^{-1} - 10^{4}$ Hz

Modelling: Source has to be included in the modelling domain

**Model parameters**: $\rho$, $\mu$, $\varepsilon$

UPPSALA UNIVERSITET

# Boundary value problem (BVP)

Total field formulation in terms of electric field $\mathbf{E}$ in frequency domain with time dependence $e^{i\omega t}$ for

- **MT**:

$$\begin{aligned} \nabla \times \frac{1}{\mu} \nabla \times \mathbf{E} + i\omega\sigma\mathbf{E} - \omega^2 \varepsilon \mathbf{E} = \mathbf{0} \quad \text{in} \quad \Omega, \\ \hat{\mathbf{n}} \times \frac{1}{-i\omega\mu} \nabla \times \mathbf{E} = \mathbf{g}_t \quad \text{on} \quad \partial\Omega, \end{aligned} \tag{1}$$

  where $\omega$ is the angular frequency and $\mathbf{g}_t = \hat{\mathbf{n}} \times \mathbf{H}_0$, $\mathbf{H}_0$ could be the plane wave magnetic field solution for a 1D or 2D background model.

- **CSEM**:

$$\begin{aligned} \nabla \times \frac{1}{\mu} \nabla \times \mathbf{E} + i\omega\sigma\mathbf{E} - \omega^2 \varepsilon \mathbf{E} = -i\omega\mathbf{J}_{source} \quad \text{in} \quad \Omega, \\ \hat{\mathbf{n}} \times \mathbf{E} = 0 \quad on \quad \partial\Omega, \end{aligned} \tag{2}$$

  where $\mathbf{J}_{source}$ describes an artificial source (e.g. electric dipole).

# Forward modelling

Compute electric and magnetic fields at receiver locations for a known model

**Workflow:**

1. Formulate BVP
2. Decide on a discretisation approach for solving the BVP numerically
3. Discretise the model domain
4. Assemble the system of equations (SOE)
5. Apply boundary conditions
6. Solve the SOE for **E** or **H** on mesh nodes or edges
7. Calculate fields at receiver stations

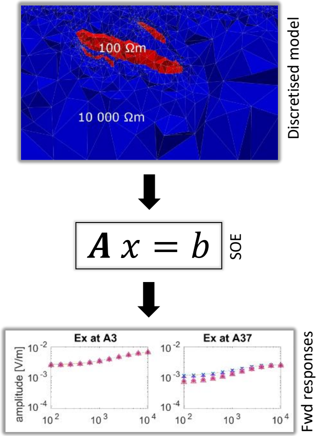

Advancing standard approaches for discretisation, boundary methods and solving the SOE

**Discretisation & boundary methods:**

- Obtain better accuracy of forward responses
- Reduce problem sizes

**Solve:**

- Reduce computational cost (time and memory) per forward solution while assuring accuracy

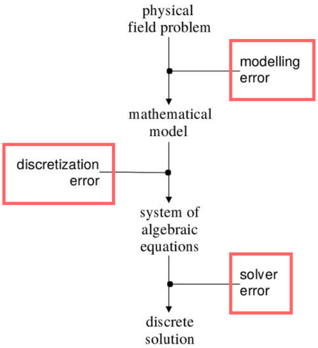


Error sources associated with the numerical solution of a field problem (Mattiussi, 2001).

UPPSALA UNIVERSITET

# Motivation

Advancing standard approaches for discretisation, boundary methods and solving the SOE

**Discretisation & boundary methods:**

- Obtain better accuracy of forward responses
- Reduce problem sizes

**Solve:**

- Reduce computational cost (time and memory) per forward solution

... to speed up the inversion process

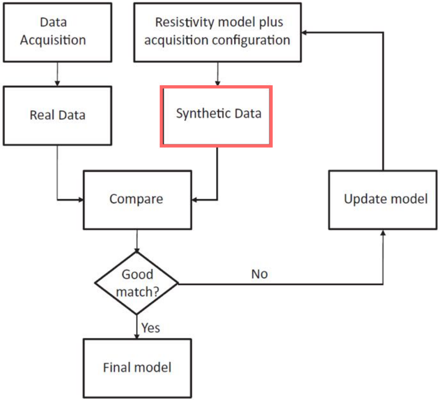


Inversion workflow (Ziolkowski and Slob, 2019)

UPPSALA UNIVERSITET

# Topics

1. Discretisation
   - Finite elements with mesh refinement
   - Spectral elements with high-order interpolation
2. Boundary Methods
   - Standard method: Dirichlet
   - Perfectly Matched Layers
3. Solving
   - Direct Solvers
   - Iterative Solvers

UPPSALA UNIVERSITET

# Topics

1. Discretisation
   - Finite elements with mesh refinement
   - Spectral elements with high-order interpolation
2. Boundary Methods
   - Standard method: Dirichlet
   - Perfectly Matched Layers
3. Solving
   - Direct Solvers
   - Iterative Solvers

UPPSALA UNIVERSITET

# Discretisation

Numerical methods for discrete approximations:

- Finite difference method (FDM)
- Method of characteristics (MOC)
- Finite element method (FEM)
- Finite volume method (FVM)
- Boundary element method (BEM)
- Meshless method (MLM)
- Spectral element method (SEM)

Commonly used element shapes $\rightarrow$ (Diersch, 2014)

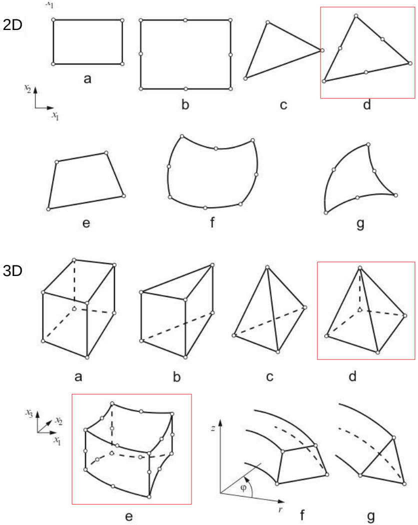


UPPSALA UNIVERSITET

## Tetrahedral FE

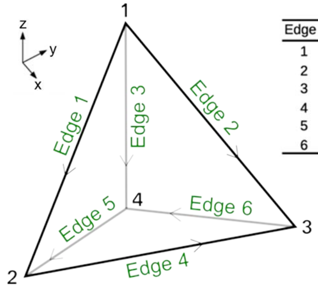


| Edge $i$ | Node $i_1$ | Node $i_2$ |
|---|---|---|
| 1 | 1 | 2 |
| 2 | 1 | 3 |
| 3 | 1 | 4 |
| 4 | 2 | 3 |
| 5 | 4 | 2 |
| 6 | 3 | 4 |

Interpolation functions: 1st order **Nédélec** (Jin, 2014)

$$\mathbf{N}_i = (L_{i1}\nabla L_{i2} - L_{i2}\nabla L_{i1})l_i$$

**Code: elfe3D** (Rulff et al., 2021) (modelling with the total **el**ectric field approach using **f**inite **e**lements in **3D**)

- Variable σ, $\mu$, ε distribution
- Customisable mesh refinement: goal-oriented adaptive, uniform global mesh quality, combination of error estimators
- Direct solver: PARDISO (Schenk and Gärtner, 2004) or MUMPS (Amestoy et al., 2001)

UPPSALA UNIVERSITET

Elements with the most inaccurate solutions are identified by high element error estimators: bisected, if they exceed a certain user-defined threshold.

**Goal-oriented adaptive refinement (h-refinement)**:

- Based on error estimators formulated for a primal and an adjoint problem (Ren et al., 2013)
- 3 optional error estimator components:
  - Residual
  - Face jumps in normal current density
  - Face jumps in tangential magnetic field

$$\begin{aligned} \eta_E^e &= \sqrt{(r_E^e)^2 + (jf_E^e)^2 + (hf_E^e)^2} \qquad (primal) \\ \eta_W^e &= \sqrt{(r_W^e)^2 + (jf_W^e)^2 + (hf_W^e)^2} \qquad (adjoint) \end{aligned} \tag{3}$$

UPPSALA UNIVERSITET

**Uniform mesh quality improvement (q-refinement)**

# Refinement

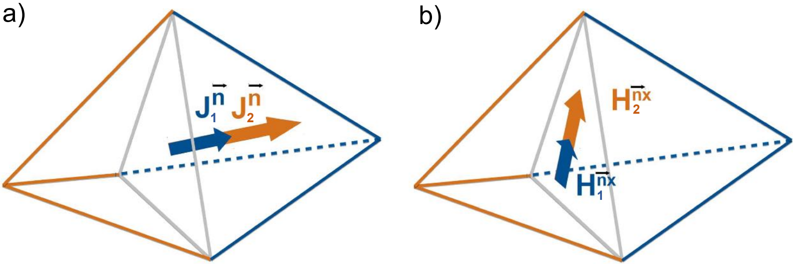


Two elements, labelled 1 and 2, sharing one face. The continuity of (a) the normal component of the current density $J^{\vec{n}}$ and (b) the tangential component of the magnetic field $\mathbf{H}^{\vec{n}\times}$ cannot be guaranteed across the common interface using an edge-based finite-element formulation for the electric field. Hence, face jumps in $J^{\vec{n}}$ and $\mathbf{H}^{\vec{n}\times}$ are used as optional terms in the error estimator guiding the mesh refinement (Rulff et al., 2021).

UPPSALA UNIVERSITET

# Refinement

Special **elfe3D** features for mesh refinement:

- Face jumps in tangential magnetic field can be included in the error estimator: helpful for models with magnetic permeability contrasts
- Refinement on low quality mesh option, increasing quality only in the last refinement step: saves time and memory
- Using average relative global error estimator $\eta_G$ and average relative error estimator at the receivers $\eta_R$ to assess refinement behaviour

$$\eta_G = \frac{1}{M}\sum_{e=1}^{M}\eta_L^e, \tag{4}$$

$$\eta_R = \frac{1}{N_r}\sum_{r=1}^{N_r}\eta_L^r, \tag{5}$$

UPPSALA UNIVERSITET

# Refinement

Special **elfe3D** features for mesh refinement:

- Source strengths in the adjoint problem take the distance to the primal source into account: ensures that all receiver locations are included equally in the error estimation
- Element error estimators are weighted with the local field strengths: avoids amplitude-dependent over-refining of the mesh

| weighting factors | decrease in $\eta_G$ | decrease in $\eta_R$ | receiver refinement | anomaly refinement | accuracy improvement |
|---|---|---|---|---|---|
| $r^3$ & amplitudes | ✓ | ✓ | ✓ | ✓ | ✓ |
| $r^3$ | ✗ | ✗ | ✗ | ✗ | ✗ |
| amplitudes | ✓ | ✗ | ✗ | ✓ | ✗ |
| none | ✗ | ✗ | ✗ | ✗ | ✓(minor) |

UPPSALA UNIVERSITET

# Example I
# FE & refinement for a synthetic block model

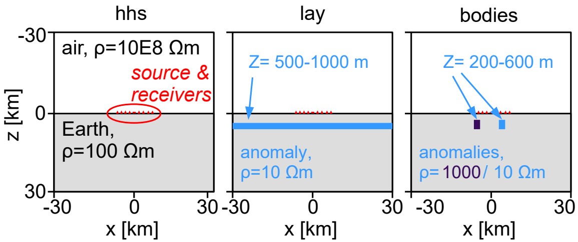


Vertical cuts of test models at $y = 0\,\mathrm{km}$. Left: homogeneous half-space model (*hhs*), middle: layered model with conductive layer (*lay*), right: model with two block anomalies (*bodies*) (Rulff et al., 2021).

**Setup:**

Source & receiver line aligned in x-direction

| | |
|---|---|
| **receiver # 1-73** | 200 to 2000 m |
| **receiver # 74-146** | -200 to -2000 m |
| **dipole source** | -50 to 50 m |

- Small source and receiver elements
- Reference solution: p2 elements with custEM (Rochlitz et al., 2019)

UPPSALA UNIVERSITET

# Example I
# FE & refinement for a synthetic block model

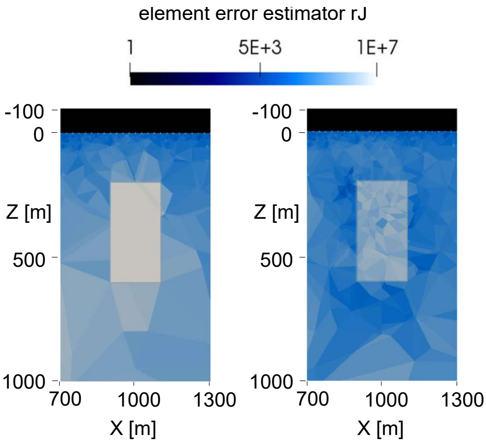


Element error estimators of the initial mesh (left) and after refinement with error estimator $rJ$ and $q = 1.6$ (right) around the conductive 3D anomaly of the model (Rulff et al., 2021).

# Example I
# FE & refinement for a synthetic block model

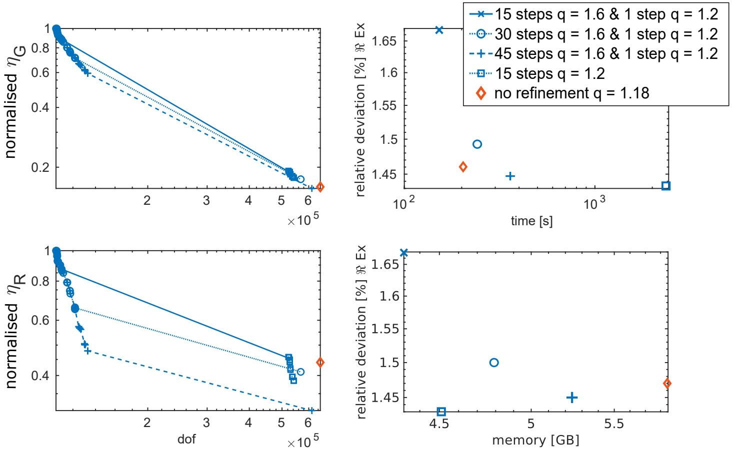


Behaviour of error estimators and computational costs (Rulff et al., 2021).

# Example II
# FE & refinement for an ore deposit model

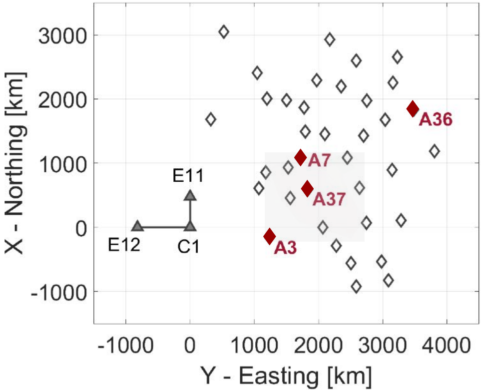


Measurement setup (Rulff et al., 2021)

**Model**

- 10 000 Ω m homogeneous half space
- Different mineral deposit resistivity scenarios (10, 100, 1 000 Ω m)
- Different values of $\mu_r$ for the mineral deposits: 1.3 or 1.0
- Frequency range: 100 Hz - 10 kHz
- Source current: 10 A

**Purpose:** detectability study

UPPSALA UNIVERSITET

# Example II
# FE & refinement for an ore deposit model

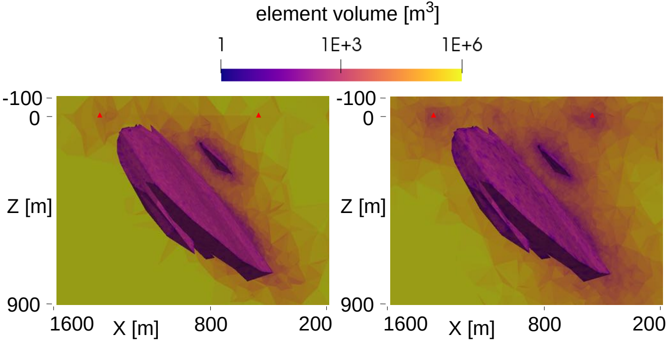


Initial and refined meshes (Rulff et al., 2021).

**Refinement**

- Magnetic mineral deposits ($\rho = 1\,000\ \Omega m$, $\mu_r = 1.3$)
- Error estimator *JH*
- Volume constraints in the complex-shaped anomalies
- Gradually increasing mesh quality factor

UPPSALA UNIVERSITET

# Example III
# FE & refinement for metallic infrastructure

**P**erfect **e**lectric **c**onductor - PEC (Alumbaugh and Newman, 1996; Um et al., 2020)

- Metallic-cased well: linewise PEC or combination of solid prism + PEC
- Implemented like a boundary condition on mesh edges corresponding to PEC
- Problem sizes are reduced & arbitrary orientation of wells possible

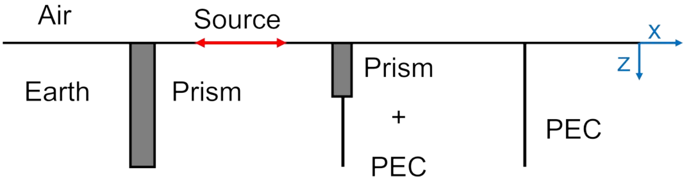


Applied options for representing a metallic-cased well
(Reyes, Rulff et al., talk O2.5.3 @ EMIW 2022)

UPPSALA UNIVERSITET

# Example III
# FE & refinement for metallic infrastructure

Model: Receiver line above basin topography crossing a metallic-cased borehole

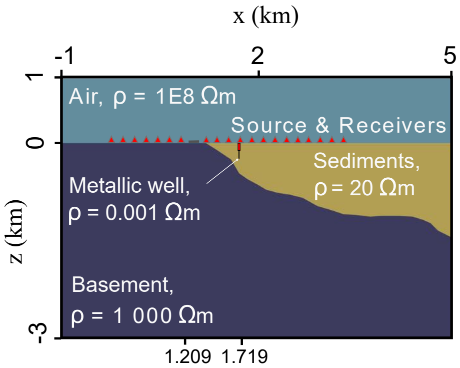


Slice through the central model region (Castillo-Reyes et al., 2023, in review)

Model parameters:

- Frequency: 2 Hz
- Receiver spacing: 25 m
- Source: in-line, 560 m distance to well
- One 200 m deep borehole

Modelling codes:

- Refinement: **elfe3D** (Rulff et al., 2021)
- Higher-order basis functions: **PETGEM** (Castillo-Reyes et al., 2018)

UPPSALA UNIVERSITET

# Example III
# FE & refinement for metallic infrastructure

**Input mesh characteristics**

- Fine source and receiver elements
- Well representation: PEC of 25 m long segments
- Mesh quality factor: q= 1.6
- 235 676 elements, 275 747 edges

**Refined mesh characteristics**

- Refined inner mesh region including PEC
- Mesh quality factor: q= 1.4
- 618 526 elements, 720 565 edges

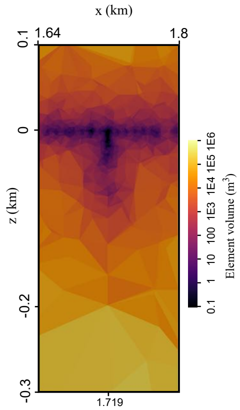


Element volumes of refined mesh at borehole location (Castillo-Reyes et al., 2023, in review)

UPPSALA UNIVERSITET

# Example III
# FE & refinement for metallic infrastructure

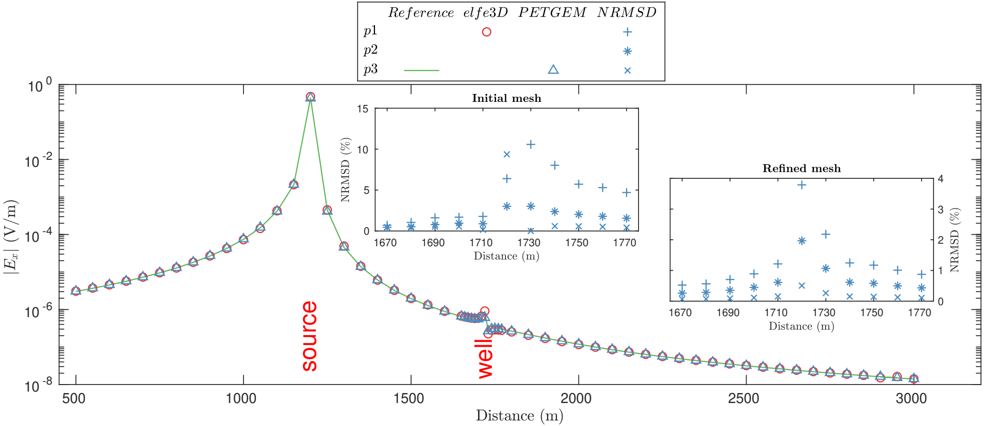


In-line electric field component (Reyes, Rulff et al., talk O2.5.3 @ EMIW 2022), reference: Castillo-Reyes et al. (2021)

UPPSALA UNIVERSITET

# Example III
# FE & refinement for metallic infrastructure

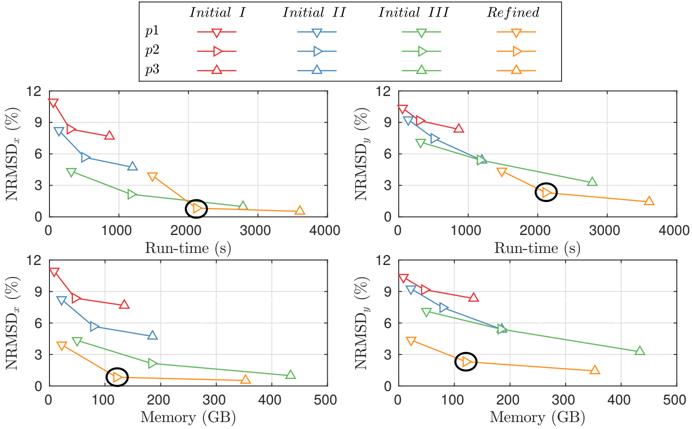


Performance summary
modified after (Castillo-Reyes et al., 2023, in review)

**Mesh qualities:**

Initial I: $q = 1.6$ (lowest)

Initial II: $q = 1.4$

Initial III: $q = 1.2$ (highest)

Refined: $q = 1.4$

PEC representation of casings, goal-oriented refinement and $p = 2$ elements work well together & produce accurate results while minimising problem sizes.

UPPSALA UNIVERSITET

**Hexahedral SE**

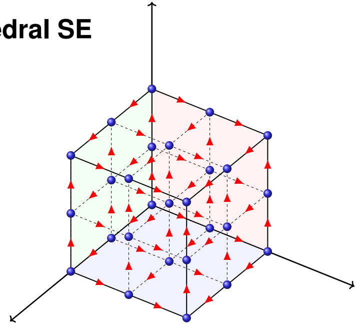

Interpolation functions: $M$-th order curl-conforming basis functions (Duruflé, 2006; Cohen and Duruflé, 2007)

$$\mathbf{N}_i^{\xi} = \phi^{(M-1)}(\xi)\phi^{(M)}(\eta)\phi^{(M)}(\zeta)\hat{\xi}$$

**Code: Spectral element code** (Weiss et al., 2023a)

- Variable $\sigma$, $\mu$ and $\varepsilon$ distributions
- Arbitrary high-order basis functions based on Lagrange polynomials defined on Gauss and Gauss-Lobatto-Legendre quadrature points
- Solver: MUMPS (Amestoy et al., 2001) or preconditioned iterative algorithm (Weiss et al., 2023b)

UPPSALA UNIVERSITET

# Example
# Buried ore body

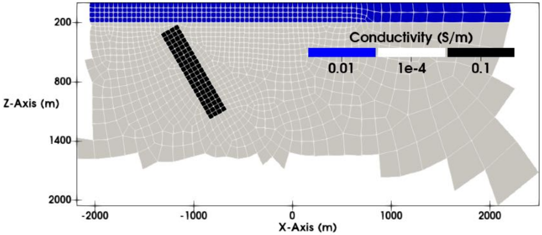


Vertical slice at $y = 0$ (Weiss et al., 2023a)

Model parameters

- Frequency: 100 Hz
- Receiver line of 4 km length with spacing of 100 m
- Source: 400 m long grounded cable perpendicular to receiver line and offset by 500 m
- 2nd order approximation

UPPSALA UNIVERSITET

# Example
# Buried ore body

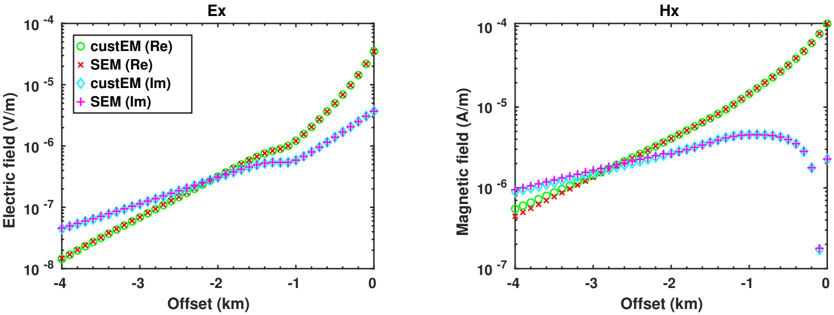


Comparison of spectral and finite element (custEM; Rochlitz et al., 2019) results (Weiss et al., 2023a)

UPPSALA UNIVERSITET

# Example
# Buried ore body

Comparison of computational quantities between the spectral and a finite element code (custEM; Rochlitz et al., 2019) based on 2nd order basis functions for the buried ore body model (cf. Weiss et al., 2023a)

| | Buried ore body model | | |
|---|---|---|---|
| | #elements | #DOF | time (s) |
| SEM | 90,714 | 2,200,218 | 1110.4 |
| custEM | 185,428 | 2,365,524 | 775 |

$\Rightarrow$ Comparable run times for comparable degrees of freedom (DOF)

$\Rightarrow$ Fewer elements required for spectral element approach

UPPSALA UNIVERSITET

# Topics

1. Discretisation
   - Finite elements with mesh refinement
   - Spectral elements with high-order interpolation
2. Boundary Methods
   - Standard method: Dirichlet
   - Perfectly Matched Layers
3. Solving
   - Direct Solvers
   - Iterative Solvers

UPPSALA UNIVERSITET

# Dirichlet BC and source implementation in 2D MT modelling

- BC should ideally **absorb/account for** all outward directed fields
- Standard: **Dirichlet BC**
  $\Longrightarrow$ Prescribed values must exactly match the 2D solution that would be computed at the boundary
- **Plane-wave source** is represented either at the anomalies or at the outer boundary
- Solution for **1D layered half space** analytically computable

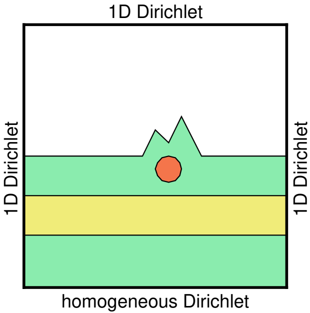


UPPSALA UNIVERSITET

# Dirichlet BC for 2D models with different sections at the left and right boundary

Option:

- Prescribe different 1D solutions at the left & right, interpolate horizontally along top
- Field correctly prescribed at sides and bottom, but only approximated at the top

$\longrightarrow$ Boundary effects from the top affect the solution in the entire domain, also at the receivers

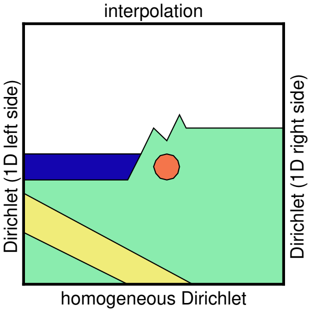


UPPSALA UNIVERSITET

# Perfectly Matched Layers

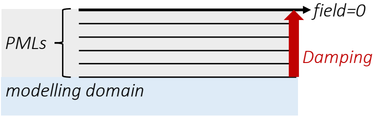


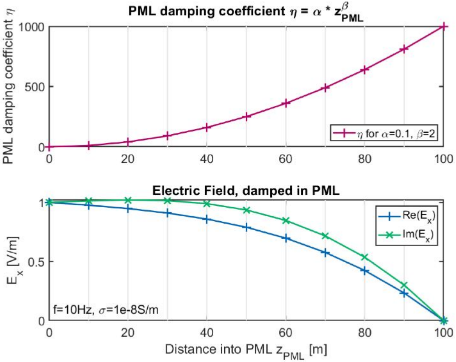


- Absorbing boundary method
- Sequence of artificial layers damping the field to zero in a **reflection-free** manner
- Outer boundary: homogeneous Dirichlet BC
- Damping coefficient: $\eta = \alpha \mid z_{\mathrm{PML}} \mid^{\beta}$
- PML may be placed closer to anomalies than Dirichlet boundaries without affecting the solution at the receivers

UPPSALA UNIVERSITET

# Total and scattered field decomposition

- PML can directly replace homogeneous Dirichlet BC in the anomalous-field approach (Rivera-Rios et al., 2019; Lei et al., 2022)
- Inhomogeneous BC cannot be directly replaced, instead, we can make use of a method called **total and scattered field decomposition** (e.g. Lou et al., 2005; Riley et al., 2006; Jin and Riley, 2008; Rumpf, 2012)
- Method originally for antenna studies, we adapted it and developed setups suitable for Earth models

UPPSALA UNIVERSITET

# Total and scattered field decomposition

**Horizontal TSFD:**

- Divide domain along horizontal interface into:
  - Total-field region: contains Earth, solution variable = total field
  - Scattered-field region: contains air layer, solution variable = scattered field
- Incident plane-wave source field excited at the TSFD interface
- PML at top, absorb the scattered field

$\Longrightarrow$ useful for realistic models with different sections at the left and right

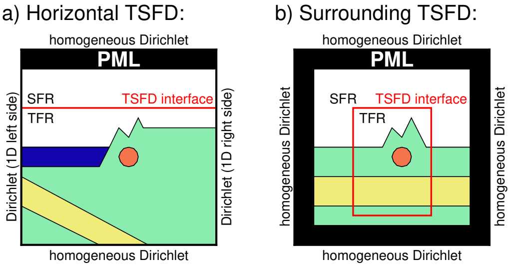


from: Buntin et al. (under review)

UPPSALA UNIVERSITET

**Surrounding TSFD:**

- Divide domain along rectangular interface into:
  - Total-field region: contains anomalies, solution variable = total field
  - Scattered-field region: contains horizontally layered background, solution variable = anomalous field
- Normal field (1D background) excited at the interface
- PML at outer boundary, absorb the anomalous field

$\Longrightarrow$ useful to shrink the domain for densely discretised high-frequency models

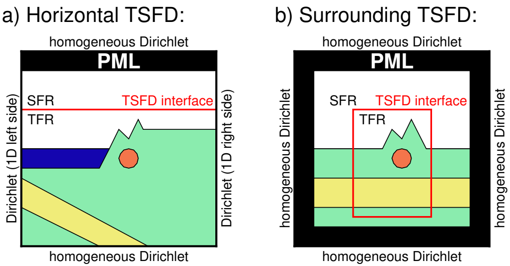


from: Buntin et al. (under review)

UPPSALA UNIVERSITET

# Total and scattered field decomposition

| | solution variable in | | |
|---|---|---|---|
| approach | SFR | TFR | TSFD interface |
| horizontal TSFD | scattered | total | incident |
| surrounding TSFD | anomalous | total | normal |

c) Elements at the TSFD interface:

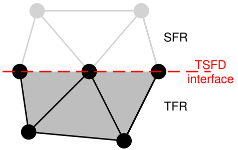


from: Buntin et al. (under review)

Jump at the TSFD interface is implemented by changing the right-hand side vector:

$$r_j = \begin{cases} -A_{jk} u_k & \text{if } j \text{ at TSFD interface, } k \text{ in SFR,} \\ +A_{jk} u_k & \text{if } j \text{ in SFR, } k \text{ at TSFD interface,} \end{cases} \tag{6}$$

$$\forall j, k = 1, 2, 3$$

where $u_k = u_k^{\text{incident}}$ (horizontal TSFD) or $u_k = u_k^{\text{normal}}$ (surrounding TSFD).

UPPSALA UNIVERSITET

# Topics

1. Discretisation
   - Finite elements with mesh refinement
   - Spectral elements with high-order interpolation
2. Boundary Methods
   - Standard method: Dirichlet
   - Perfectly Matched Layers
3. Solving
   - Direct Solvers
   - Iterative Solvers

UPPSALA UNIVERSITET

# Solution techniques for systems of equations (SOE)

Linear SOE can be solved using either direct or iterative solvers

Direct solvers

- Very robust and easy to use
- Time and memory complexities of sparse direct solver are $\mathcal{O}(N^2)$ and $\mathcal{O}(N^{4/3})$ in 3D
- Non-optimal scalability

$\Rightarrow$ Use computer clusters to avoid memory bottle neck

Iterative solvers

- Lack robustness
- Only need storage for non-zero entries of system matrix and several additional vectors
- Rely on easily scalable matrix-vector multiplications and vector operations

$\Rightarrow$ Use preconditioning to ensure robustness and improve convergence rate

UPPSALA UNIVERSITET

Rewrite complex-valued SOE

$$\left(\mathbf{K} + i\mathbf{M}_\sigma - \mathbf{M}_\varepsilon\right)\mathbf{E} = \mathbf{b},$$

as real-equivalent two-by-two system of form

$$\underbrace{\begin{bmatrix} \mathbf{M}_\sigma & -(\mathbf{K} - \mathbf{M}_\varepsilon) \\ \mathbf{K} - \mathbf{M}_\varepsilon & \mathbf{M}_\sigma \end{bmatrix}}_{\mathbf{C}_{\mathbf{RI}}} \begin{bmatrix} \mathbf{E}_\mathbf{R} \\ -\mathbf{E}_\mathbf{I} \end{bmatrix} = \begin{bmatrix} \mathbf{b}_\mathbf{I} \\ \mathbf{b}_\mathbf{R} \end{bmatrix},$$

UPPSALA UNIVERSITET

# PREconditioning for Square Blocks: PRESB

PRESB is a robust and efficient preconditioner for two-by-two block systems of general form

$$\mathcal{A} = \begin{bmatrix} \mathbf{A} & -b\,\mathbf{B}_2 \\ a\mathbf{B}_1 & \mathbf{A} \end{bmatrix},$$

with the assumption that **A** is **symmetric positive definite.** PRESB reads as follows

$$\mathcal{P} = \begin{bmatrix} \mathbf{A} & -\mathbf{B}_2 \\ \mathbf{B}_1 & \mathbf{A} + \sqrt{ab}(\mathbf{B}_1 + \mathbf{B}_2) \end{bmatrix}$$

and it can be proved that all the eigenvalues of the preconditioned system $\mathcal{P}^{-1}\mathcal{A}$ are clustered in the interval $[\frac{1}{2}, 1]$, **independently of the discretisation and material parameters** and the scalars $a$ and $b$ (see Axelsson et al., 2016).

UPPSALA UNIVERSITET

To solve

$$\begin{bmatrix} \mathbf{M}_\sigma & -(\mathbf{K}-\mathbf{M}_\varepsilon) \\ \mathbf{K}-\mathbf{M}_\varepsilon & \mathbf{M}_\sigma \end{bmatrix} \begin{bmatrix} \mathbf{E_R} \\ -\mathbf{E_I} \end{bmatrix} = \begin{bmatrix} \mathbf{b_I} \\ \mathbf{b_R} \end{bmatrix}$$

the Generalized Conjugate Residual (GCR) method is applied. To precondition this system, PRESB is taken as preconditioner

$$\mathbf{P} = \begin{bmatrix} \mathbf{M}_\sigma & -(\mathbf{K}-\mathbf{M}_\varepsilon) \\ \mathbf{K}-\mathbf{M}_\varepsilon & \mathbf{M}_\sigma + 2(\mathbf{K}-\mathbf{M}_\varepsilon) \end{bmatrix}.$$

UPPSALA UNIVERSITET

The computations of applying the PRESB preconditioner, that is solving a system of form

$$\mathbf{P}\begin{bmatrix}\mathbf{w_1}\\ \mathbf{w_2}\end{bmatrix} = \begin{bmatrix}\mathbf{f_1}\\ \mathbf{f_2}\end{bmatrix},$$

consists of performing the following steps:

**Algorithm 1:** Solving linear system with preconditioner $\mathbf{P}$

1. Set $\mathbf{H} = \mathbf{M}_\sigma + (\mathbf{K} - \mathbf{M}_\varepsilon)$
2. Solve $\mathbf{Hg} = \mathbf{f_1} + \mathbf{f_2}$
3. Compute $\mathbf{M}_\sigma\mathbf{g}$ and $\mathbf{f_1} - \mathbf{M}_\sigma\mathbf{g}$
4. Solve $\mathbf{Hh} = \mathbf{f_1} - \mathbf{M}_\sigma\mathbf{g}$
5. Compute $\mathbf{w_1} = \mathbf{g} + \mathbf{h}$ and $\mathbf{w_2} = -\mathbf{h}$

UPPSALA UNIVERSITET

# Iterative algorithm

**Algorithm 2:** Iterative framework

**Input:** $\mathbf{C_{RI}}, \mathbf{b}, \mathbf{H}, \mathbf{M}_\sigma$, tol

**Output:** $\mathbf{E}$

```
Let x_0 be the initial guess
Set r_0 = b − C_RI x_0
for i = 0, ... m do
    Compute p_i using Algorithm 1 with r_i being the right hand side
    q_i ← C_RI p_i
    q_i ← q_i − Σ_{j=0}^{i−1} q_j (q_i, q_j)/(q_j, q_j)
    p_i ← p_i − Σ_{j=0}^{i−1} p_j (q_i, q_j)/(q_j, q_j)
    al_i ← (r_i, q_i)/(q_i, q_i)
    x_{i+1} ← x_i + al_i p_i
    r_{i+1} ← r_i − al_i q_i
    if ||r_{i+1}||_2 / ||b||_2 < tol then Stop

end
```

$$\mathbf{x}_0 \text{ initial guess}, \quad \mathbf{r}_0 = \mathbf{b} - \mathbf{C_{RI}}\mathbf{x}_0$$

$$\mathbf{q}_i \leftarrow \mathbf{C_{RI}}\mathbf{p}_i$$

$$\mathbf{q}_i \leftarrow \mathbf{q}_i - \sum_{j=0}^{i-1} \mathbf{q}_j \frac{(\mathbf{q}_i, \mathbf{q}_j)}{(\mathbf{q}_j, \mathbf{q}_j)}$$

$$\mathbf{p}_i \leftarrow \mathbf{p}_i - \sum_{j=0}^{i-1} \mathbf{p}_j \frac{(\mathbf{q}_i, \mathbf{q}_j)}{(\mathbf{q}_j, \mathbf{q}_j)}$$

$$al_i \leftarrow \frac{(\mathbf{r}_i, \mathbf{q}_i)}{(\mathbf{q}_i, \mathbf{q}_i)}$$

$$\mathbf{x}_{i+1} \leftarrow \mathbf{x}_i + al_i \mathbf{p}_i$$

$$\mathbf{r}_{i+1} \leftarrow \mathbf{r}_i - al_i \mathbf{q}_i$$

$$\text{if } \frac{||\mathbf{r}_{i+1}||_2}{||\mathbf{b}||_2} < tol \text{ then Stop}$$

UPPSALA UNIVERSITET

# Implementation

- Code written in Fortran
- Implemented in a parallel fashion using Message Passing Interface (MPI)
- Relying on functionalities of open-source libraries PETSc (Balay et al., 1997, 2022), MUMPS (Amestoy et al., 2001, 2006) and hypre (Falgout and Yang, 2002; Falgout et al., 2006).
- Outer-inner solution method
- Outer solver: GCR preconditioned with PRESB
- Inner solver: GCR or flexible generalised minimal residual (FGMRES) method preconditioned with the auxiliary-space Maxwell solver (AMS; Kolev and Vassilevski, 2006, 2009; Grayver and Kolev, 2015)

UPPSALA UNIVERSITET

# Test models

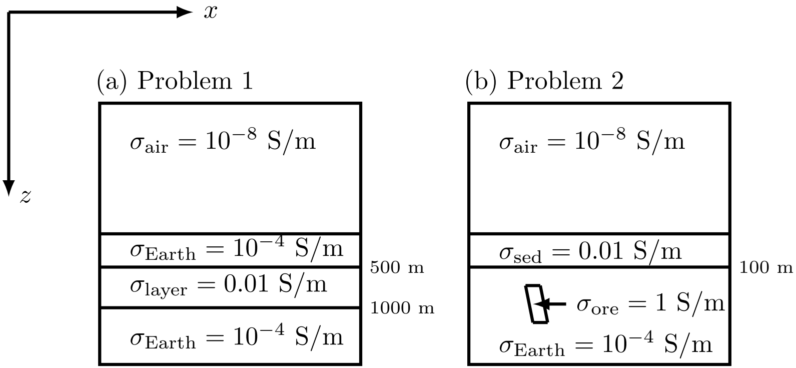


Schematic side views (Weiss et al., 2023b)

UPPSALA UNIVERSITET

# Test models

Model information (see Weiss et al., 2023b)

| Model | Layered Earth | 3-D model |
|---|---|---|
| Domain size [km$^3$] | $30 \times 30 \times 30$ | $30 \times 36 \times 30$ |
| Conductivities [S/m] | $\sigma_{\text{Air}} = 10^{-8}$, $\sigma_{\text{Earth}} = 10^{-4}$, $\sigma_{\text{Layer}} = 10^{-2}$ | $\sigma_{\text{Air}} = 10^{-8}$, $\sigma_{\text{Earth}} = 10^{-4}$, $\sigma_{\text{cover}} = 0.01$, $\sigma_{\text{ore}} = 1$ |
| Approximation order | 1st | 1st |
| # elements | $54 \times 54 \times 54$ | 332’580 |
| # degrees of freedom | 980’100 | 2’033’986 |

- Runs performed on AMD Ryzen Threadripper 2950X 16-core processor clocked at 3.5 GHz and with 128 GB RAM
- Run with two MPI processes

UPPSALA UNIVERSITET

# Robustness of solver with respect to frequency

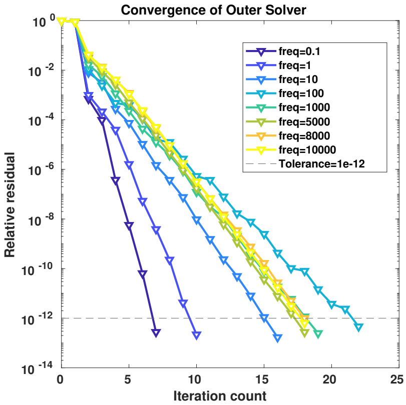


Convergence of outer solver (Weiss et al., 2023b)

UPPSALA UNIVERSITET

# Robustness of solver with respect to frequency

Computational quantities for the **layered Earth model** and variable frequencies for edge elements of degree $p = 1$. The number of outer GCR iterations is denoted by $N_{it}^{outer}$ (Weiss et al., 2023b)

| Inner solver | AMS-GCR | | | AMS-FGMRES | | | DMUMPS | | |
|---|---|---|---|---|---|---|---|---|---|
| freq [Hz] | $N_{it}^{outer}$ | time [s] | mem [GB] | $N_{it}^{outer}$ | time [s] | mem [GB] | $N_{it}^{outer}$ | time [s] | mem [GB] |
| 0.1 | 7 | 40.0 | **4.3** | 7 | 39.3 | **4.3** | 6 | 121.8 | **14.1** |
| 1 | 10 | 56.7 | 4.4 | 10 | 55.8 | 4.3 | 9 | 147.3 | 14.1 |
| 10 | 16 | 79.3 | 4.4 | 16 | 78.3 | 4.4 | 15 | 145.3 | 14.0 |
| 100 | 22 | 93.5 | 4.5 | 22 | 92.7 | 4.3 | 18 | 157.2 | 14.1 |
| 1000 | 19 | 70.2 | 4.4 | 19 | 69.3 | 4.3 | 17 | 166.7 | 14.0 |
| 5000 | 18 | 62.8 | 4.4 | 18 | 62.1 | 4.3 | 17 | 153.0 | 14.0 |
| 8000 | 18 | 96.8 | 4.4 | 18 | 95.6 | 4.4 | 18 | 157.8 | 14.2 |
| 10000 | 18 | **460.7** | 4.4 | 18 | **443.4** | 4.4 | 18 | **168.7** | 14.1 |

UPPSALA UNIVERSITET

# Robustness of solver with respect to frequency

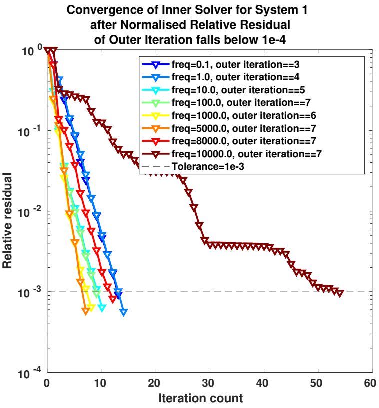


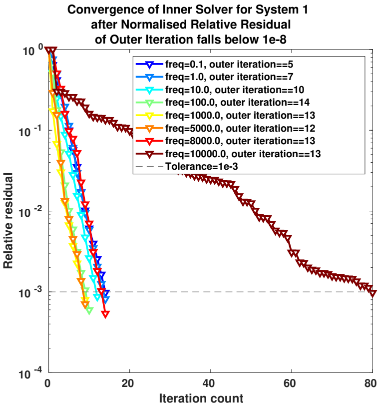


Convergence curves of the inner AMS-preconditioned GCR solver for the first inner system (Steps 1 of Algorithm 1) when the normalised relative residual of the outer solver reaches values of $10^{-4}$ and $10^{-8}$ (Weiss et al., 2023b)

UPPSALA UNIVERSITET

# Robustness of solver with respect to problem size

Comparison of outer iteration counts ($N_{it}^{outer}$) and solving times (time [s]) for various frequencies and problem sizes **for the layered Earth model** (Weiss et al., 2023b)

| | frequency [Hz] | | | | | | | |
|---|---|---|---|---|---|---|---|---|
| | 0.1 | | 10 | | 1000 | | 8000 | |
| #DOF | $N_{it}^{outer}$ | time[s] | $N_{it}^{outer}$ | time[s] | $N_{it}^{outer}$ | time[s] | $N_{it}^{outer}$ | time[s] |
| 980'100 | 7 | 42.2 | 16 | 79.3 | 19 | 70.2 | 18 | 96.8 |
| 3'641'400 | 8 | 152.9 | 15 | 286.4 | 18 | 272.6 | 19 | 310.2 |
| 6'879'600 | 8 | 343.4 | 16 | 646.5 | 18 | 521.8 | 18 | 790.5 |

- Stable outer iteration count with respect to problem size
- Time increases about linearly

UPPSALA UNIVERSITET

# Robustness of solver with respect to permeability

Comparison of outer iteration counts ($N_{it}^{outer}$) and solving times (time [s]) for various frequencies and different magnetic permeability values for the ore body of the **3D** model (Weiss et al., 2023b)

| | relative magnetic permeability $\mu_r$ of ore body | | | | | | | |
|---|---|---|---|---|---|---|---|---|
| | 1 | | 2 | | 5 | | 10 | |
| frequency [Hz] | $N_{it}^{outer}$ | time[s] | $N_{it}^{outer}$ | time[s] | $N_{it}^{outer}$ | time[s] | $N_{it}^{outer}$ | time[s] |
| 0.1 | 9 | 594.5 | 9 | 586.0 | 10 | 656.7 | 11 | 691.8 |
| 10 | 16 | 284.8 | 16 | 282.3 | 16 | 180.1 | 16 | 279.2 |
| 100 | 23 | 278.6 | 23 | 275.4 | 23 | 273.7 | 24 | 284.1 |
| 8000 | 18 | 324.3 | 18 | 345.0 | 18 | 344.7 | 18 | 331.4 |

UPPSALA UNIVERSITET

# Robustness of solver with respect to permeability & permittivity

Comparison of iteration counts ($N_{it}^{outer}$) and solving times (time [s]) for various frequencies. Note that these simulations are run with a variable dielectric permittivity distribution and two different magnetic permeability values for the ore body of the **3D model** (Weiss et al., 2023b)

| relative dielectric permittivity of air, cover, host rock and ore body | $\varepsilon_r^{air} = 1$, $\varepsilon_r^{cover} = 20$, $\varepsilon_r^{host\ rock} = 5$, $\varepsilon_r^{ore\ body} = 1$ | | | |
|---|---|---|---|---|
| relative magnetic permeability of ore body | $\mu_r = 1$ | | $\mu_r = 10$ | |
| frequency [Hz] | $N_{it}^{outer}$ | time[s] | $N_{it}^{outer}$ | time[s] |
| 0.1 | 9 | 590.4 | 11 | 691.6 |
| 10 | 16 | 282.3 | 16 | 279.8 |
| 100 | 23 | 278.5 | 24 | 285.1 |
| 8000 | 18 | 341.0 | 18 | 322.4 |

UPPSALA UNIVERSITET

# Iterative or direct solver?

Computational comparisons of iterative and direct solvers in terms of time and memory consumption for the **layered Earth model** at a frequency of 100 Hz for different problem sizes (Weiss et al., 2023b)

| | Iterative Method: GCR | | | | Direct Solver: ZMUMPS | |
|---|---|---|---|---|---|---|
| Inner solver | Preconditioned GCR | | DMUMPS | | - | |
| #DOF | time[s] | mem[GB] | time[s] | mem[GB] | time[s] | mem[GB] |
| 980’100 | 93.5 | 4.4 | 157.2 | 14.1 | 166.8 | 9.0 |
| 3’641’400 | 368.4 | 16.4 | 1625.0 | 74.8 | 1874.1 | 55.5 |
| 6’879’600 | 661.0 | 30.1 | - | out of memory | - | out of memory |

- Iterative solver requires far less memory than direct solver
- Iterative framework also needs less time to solve linear system of equations

UPPSALA UNIVERSITET

# Take aways

## Technical insights into advanced numerical methods applied in 3D EM modelling

Geophysical Journal International

*Geophys. J. Int.* (2021) **227,** 1624–1645 https://doi.org/10.1093/gji/ggab264
Advance Access publication 2021 July 08
GJI General Geophysical Methods

**Efficient goal-oriented mesh refinement in 3-D finite-element modelling adapted for controlled source electromagnetic surveys**

Paula Rulff, Laura M. Buntin and Thomas Kalscheuer
*Department of Earth Sciences, Uppsala University, Uppsala, 75236, Sweden. E-mail: paula.rulff@geo.uu.se*

Accepted 2021 July 6. Received 2021 June 28; in original form 2020 July 2

Geophysical Journal International

*Geophys. J. Int.* (2023) **232,** 1427–1454 https://doi.org/10.1093/gji/ggac358
Advance Access publication 2022 September 11
GJI Geomagnetism, Rock Magnetism and Palaeomagnetism

**Spectral element method for 3-D controlled-source electromagnetic forward modelling using unstructured hexahedral meshes**

M. Weiss,[1] T. Kalscheuer[1] and Z. Ren[2]
[1] *Department of Earth Sciences, Uppsala University, 752 36 Uppsala, Sweden. E-mail: michael.weiss@geo.uu.se*
[2] *School of Geosciences and Info-Physics, Central South University, Changsha, Hunan 410083, China*

Accepted 2022 September 7. Received 2022 August 25; in original form 2022 January 25

**Improved accuracy of plane-wave electromagnetic modelling by application of the total and scattered field decomposition and perfectly matched layers**

L.M. Buntin[1], T. Kalscheuer[1], G. Kreiss[2], Z. Ren[3]
[1] *Dept. of Earth Sciences, Uppsala University, Uppsala, Sweden*
[2] *Dept. of Information Technology, Uppsala University, Uppsala, Sweden*
[3] *School of Geo-science and Info-Physics, Central South University, Changsha, China*

In review @ GJI

Computational Geosciences
https://doi.org/10.1007/s10596-022-10182-2

ORIGINAL PAPER

Check for updates

**Iterative solution methods for 3D controlled-source electromagnetic forward modelling of geophysical exploration scenarios**

Michael Weiss[1] · Maya Neytcheva[2] · Thomas Kalscheuer[1]

Received: 30 June 2022 / Accepted: 7 November 2022
© The Author(s) 2022

# Acknowledgements

We would like to thank:

- Thomas Kalscheuer, Maya Neytcheva, Gunilla Kreiss and Zhengyong Ren for supervision
- The EM community for good feedback at conferences
- The reviewers of our articles
- Our funding sources:

- MTnet and the EMinar team ☺

# Contributions

**Laura Buntin**
laura.buntin@geo.uu.se

- MT FE modelling
- Boundary methods
- TSFD

**Michael Weiss**
weissmilu@gmail.com

- CSEM SE modelling
- Iterative solution methods

**Paula Rulff**
paula.rulff@geo.uu.se

- CSEM FE modelling
- Mesh refinement
- Inversion

UPPSALA UNIVERSITET

# References I


Alumbaugh, D. L. and Newman, G. A. (1996). Electromagnetic modeling of perfect conductors in an arbitrary host. In *1996 SEG Annual Meeting*. OnePetro.

Amestoy, P. R., Duff, I. S., L'Excellent, J.-Y., and Koster, J. (2001). A fully asynchronous multifrontal solver using distributed dynamic scheduling. *SIAM Journal on Matrix Analysis and Applications*, 23(1):15–41.

Amestoy, P. R., Guermouche, A., L'Excellent, J.-Y., and Pralet, S. (2006). Hybrid scheduling for the parallel solution of linear systems. *Parallel Computing*, 32(2):136–156.

Axelsson, O., Farouq, S., and Neytcheva, M. (2016). Comparison of preconditioned Krylov subspace iteration methods for PDE-constrained optimization problems. *Numerical Algorithms*, 73(3):631–663.

Balay, S., Abhyankar, S., Adams, M. F., Benson, S., Brown, J., Brune, P., Buschelman, K., Constantinescu, E., Dalcin, L., Dener, A., Eijkhout, V., Gropp, W. D., Hapla, V., Isaac, T., Jolivet, P., Karpeev, D., Kaushik, D., Knepley, M. G., Kong, F., Kruger, S., May, D. A., McInnes, L. C., Mills, R. T., Mitchell, L., Munson, T., Roman, J. E., Rupp, K., Sanan, P., Sarich, J., Smith, B. F., Zampini, S., Zhang, H., Zhang, H., and Zhang, J. (2022). PETSc/TAO users manual. Technical Report ANL-21/39 - Revision 3.17, Argonne National Laboratory.

Balay, S., Gropp, W. D., McInnes, L. C., and Smith, B. F. (1997). Efficient management of parallelism in object oriented numerical software libraries. In Arge, E., Bruaset, A. M., and Langtangen, H. P., editors, *Modern Software Tools in Scientific Computing*, pages 163–202. Birkhäuser Press.


UPPSALA UNIVERSITET

Bücker, M., García, S. L., Guerrero, B. O., Caballero, M., Pérez, L., Caballero, L., de la Paz, C. P., Sánchez-Galindo, A., Villegas, F. J., Orozco, A. F., Brown, E., Werne, J., Garcés, B. V., Schwalb, A., Kemna, A., Sánchez-Alvaro, E., Launizar-Martínez, N., Valverde-Placencia, A., and Garay-Jiménez, F. (2017). Geoelectrical and electromagnetic methods applied to paleolimnological studies: Two examples from desiccated lakes in the Basin of Mexico. *Boletin de la Sociedad Geologica Mexicana*, 69(2):279–298.

Castillo-Reyes, O., de la Puente, J., and Cela, J. M. (2018). PETGEM: A parallel code for 3D CSEM forward modeling using edge finite elements. *Computers and Geosciences*, 119:123–136.

Castillo-Reyes, O., Queralt, P., Marcuello, A., and Ledo, J. (2021). Land CSEM simulations and experimental test using metallic casing in a geothermal exploration context: Vallès basin (NE Spain) case study. *IEEE Transactions on Geoscience and Remote Sensing*, 60:1–13.

Castillo-Reyes, O., Rulff, P., Schankee Um, E., and Amor-Martin, A. (2023). Meshing strategies for 3D geo-electromagnetic modelling in the presence of metallic infrastructure. *under revision in Computational Geosciences*.

Cohen, G. and Duruflé, M. (2007). Non spurious spectral-like element methods for Maxwell's equations. *Journal of Computational Mathematics*, pages 282–304.


UPPSALA UNIVERSITET

# References III


Diersch, H.-J. G. (2014). *Fundamental Concepts of Finite Element Method (FEM)*. Springer Berlin Heidelberg, Berlin, Heidelberg.

Duruflé, M. (2006). *Intégration numérique et éléments finis d'ordre élevé appliqués aux équations de Maxwell en régime harmonique*. PhD thesis, ENSTA ParisTech.

Falgout, R. D., Jones, J. E., and Yang, U. M. (2006). The design and implementation of hypre, a library of parallel high performance preconditioners. In *Numerical Solution of Partial Differential Equations on Parallel Computers*, pages 267–294. Springer.

Falgout, R. D. and Yang, U. M. (2002). hypre: A library of high performance preconditioners. In *International Conference on Computational Science*, pages 632–641. Springer.

Grayver, A. V. and Kolev, T. V. (2015). Large-scale 3D geoelectromagnetic modeling using parallel adaptive high-order finite element methodEM modeling with high-order FEM. *Geophysics*, 80(6):E277–E291.

Jin, J. and Riley, D. J. (2008). *Finite Element Analysis of Antennas and Arrays*. Wiley.

Jin, J.-M. (2014). *The finite element method in electromagnetics*. John Wiley & Sons.

Kolev, T. V. and Vassilevski, P. (2006). Parallel H1-based auxiliary space AMG solver for H (curl) problems. Technical report, Lawrence Livermore National Lab.(LLNL), Livermore, CA (United States).


UPPSALA UNIVERSITET

# References IV


Kolev, T. V. and Vassilevski, P. S. (2009). Parallel auxiliary space AMG for H (curl) problems. *Journal of Computational Mathematics*, pages 604–623.

Lei, D., Yang, L., Fu, C., Wang, R., and Wang, Z. (2022). The application of a novel perfectly matched layer in magnetotelluric simulations. *Geophysics*, 87(3):E163–E175.

Lou, Z., Petersson, L. R., Jin, J.-M., and Riley, D. J. (2005). Total-and scattered-field decomposition technique for the finite-element time-domain modeling of buried scatterers. *IEEE Antennas and Wireless Propagation Letters*, 4:133–137.

Mattiussi, C. (2001). The finite volume, finite difference, and finite elements methods as numerical methods for physical field problems.

Ren, Z., Kalscheuer, T., Greenhalgh, S., and Maurer, H. (2013). A goal-oriented adaptive finite-element approach for plane wave 3-D electromagnetic modelling. *Geophysical Journal International*, 194(2):700–718.

Riley, D. J., Jin, J.-M., Lou, Z., and Petersson, L. R. (2006). Total-and scattered-field decomposition technique for the finite-element time-domain method. *IEEE transactions on antennas and propagation*, 54(1):35–41.

Rivera-Rios, A. M., Zhou, B., Heinson, G., and Krieger, L. (2019). Multi-order vector finite element modeling of 3D magnetotelluric data including complex geometry and anisotropy. *Earth, Planets and Space*, 71(1):1–25.


UPPSALA UNIVERSITET

# References V


Rochlitz, R., Skibbe, N., and Günther, T. (2019). custEM: Customizable finite-element simulation of complex controlled-source electromagnetic data. *Geophysics*, 84(2):F17–F33.

Rulff, P., Buntin, L. M., and Kalscheuer, T. (2021). Efficient goal-oriented mesh refinement in 3D finite-element modelling adapted for controlled-source electromagnetic surveys across ferrous mineral deposits. *Geophysical Journal International*, 227(3):1624–1645.

Rumpf, R. C. (2012). Simple implementation of arbitrarily shaped total-field/scattered-field regions in finite-difference frequency-domain. *Progress In Electromagnetics Research*, 36:221–248.

Schenk, O. and Gärtner, K. (2004). Solving unsymmetric sparse systems of linear equations with pardiso. *Future Generation Computer Systems*, 20(3):475–487.

Um, E. S., Kim, J., and Wilt, M. (2020). 3D borehole-to-surface and surface electromagnetic modeling and inversion in the presence of steel infrastructure. *Geophysics*, 85(5):E139–E152.

Weiss, M., Kalscheuer, T., and Ren, Z. (2023a). Spectral element method for 3-D controlled-source electromagnetic forward modelling using unstructured hexahedral meshes. *Geophysical Journal International*, 232(2):1427–1454.

Weiss, M., Neytcheva, M., and Kalscheuer, T. (2023b). Iterative solution methods for 3D controlled-source electromagnetic forward modelling of geophysical exploration scenarios. *Computational Geosciences*, 27:81–102.

Ziolkowski, A. and Slob, E. (2019). *Introduction to Controlled-Source Electromagnetic Methods*. Cambridge University Press.